DTIC FILE COPY

Unclas
SECURITY C

AD-A223 997

DTIC ELECTE JUN 29 1990 S D

REPORT DOCUMENTATION PAGE

Form Approved
OMB No. 0704-0188

1a. REPORT SECURITY CLASSIFICATION: Unclassified	1b. RESTRICTIVE MARKINGS
2a. SECURITY CLASSIFICATION AUTHORITY	3. DISTRIBUTION/AVAILABILITY OF REPORT: Approved for Public Release; Distribution unlimited
2b. DECLASSIFICATION/DOWNGRADING SCHEDULE	
4. PERFORMING ORGANIZATION REPORT NUMBER(S): GL-TR-90-0150	5. MONITORING ORGANIZATION REPORT NUMBER(S)
6a. NAME OF PERFORMING ORGANIZATION: Geophysics Laboratory; 6b. OFFICE SYMBOL (If applicable): PHS	7a. NAME OF MONITORING ORGANIZATION
6c. ADDRESS (City, State, and ZIP Code): Hanscom AFB, Massachusetts 01731-5000	7b. ADDRESS (City, State, and ZIP Code)
8a. NAME OF FUNDING/SPONSORING ORGANIZATION; 8b. OFFICE SYMBOL (If applicable)	9. PROCUREMENT INSTRUMENT IDENTIFICATION NUMBER
8c. ADDRESS (City, State, and ZIP Code)	10. SOURCE OF FUNDING NUMBERS: PROGRAM ELEMENT NO 61102F; PROJECT NO 2311; TASK NO G3; WORK UNIT ACCESSION NO 12

11. TITLE (Include Security Classification): Magnetoconvection on the Solar Surface

12. PERSONAL AUTHOR(S): George W. Simon

13a. TYPE OF REPORT	13b. TIME COVERED	14. DATE OF REPORT (Year, Month, Day)	15. PAGE COUNT
Reprint	FROM _____ TO _____	1990 June 20	12

16. SUPPLEMENTARY NOTATION: Reprinted from Physics of Space Plasmas, ed. T. Chang, Scientific Publishers, Cambridge, MA October 1989

17. COSATI CODES		
FIELD	GROUP	SUB-GROUP

18. SUBJECT TERMS (Continue on reverse if necessary and identify by block number): Solar convection, Solar magnetic fields, Spacelab 2

19. ABSTRACT (Continue on reverse if necessary and identify by block number)

The solar surface is the astrophysicist's best laboratory for the study of magnetoconvection. Here exists equipartition of magnetic and kinetic energy. Higher up in the thin atmosphere of the solar corona, the gas is "frozen" into the magnetic field lines, while below the surface the field must follow the motions of much denser ionized gas. First we give a historical review of observations of small-scale solar magnetic fields and convective flows, and then show remarkable new results obtained by "seeing-free" (without distortion) cinematography of the solar surface from NASA's Spacelab 2 mission. Not only do we see systematic outflows from sunspots, but also the quiet Sun appears to be covered by convective sources, sinks, and vortices. Simultaneously-obtained magnetic field motions show excellent correlation with the gas flows. We describe a simple kinematical model for these motions, and discuss briefly the implication of these data for the study of flares.

Solar convection; magnetic fields; Solar flares. (CP)
keywords: reprints;

20. DISTRIBUTION/AVAILABILITY OF ABSTRACT	21. ABSTRACT SECURITY CLASSIFICATION
☐ UNCLASSIFIED/UNLIMITED ☒ SAME AS RPT. ☐ DTIC USERS	Unclassified

22a. NAME OF RESPONSIBLE INDIVIDUAL	22b. TELEPHONE (Include Area Code)	22c. OFFICE SYMBOL
Claire Caulfield	(617) 377-4555	GL/SULLP

DD Form 1473, JUN 86 — Previous editions are obsolete. — SECURITY CLASSIFICATION OF THIS PAGE: Unclassified

90 06 27 125

GL-TR-90-0150

PHYSICS OF SPACE PLASMAS (1988)
SPI Conference Proceedings and Reprint Series, Vol. 8

MAGNETOCONVECTION ON THE SOLAR SURFACE

George W. Simon
Air Force Geophysics Laboratory, Sunspot, New Mexico 88349

ABSTRACT

The solar surface is the astrophysicist's best laboratory for the study of magnetoconvection. Here exists equipartition of magnetic and kinetic energy. Higher up in the thin atmosphere of the solar corona, the gas is "frozen" into the magnetic field lines, while below the surface the field must follow the motions of much denser ionized gas. First we give a historical review of observations of small-scale solar magnetic fields and convective flows, and then show remarkable new results obtained by "seeing-free" (without distortion) cinematography of the solar surface from NASA's Spacelab 2 mission. Not only do we see systematic outflows from sunspots, but also the quiet Sun appears to be covered by convective sources, sinks, and vortices. Simultaneously-obtained magnetic field motions show excellent correlation with the gas flows. We describe a simple kinematical model for these motions, and discuss briefly the implication of these data for the study of flares.

I. BACKGROUND: THE SOLAR PHOTOSPHERE

With even a relatively small telescope, say one having a 25-30 cm diameter objective lens, it is possible to see that the surface of the Sun is covered by a grainy-looking structure, which is called granulation (Fig. 1). Granules are convection bubbles, typically having a size of 1 Mm (about the size of Texas) and a lifetime of 10 to 20 min. Most of the Sun's heat transport through its outer layers to the surface is by convection. We call the Sun's visible surface layer the photosphere (light sphere). The roundish black object in Fig. 1 is a sunspot (this one has just the diameter of the Earth -- i.e., about one percent of the solar diameter). It is not really black, but appears so because it is about 2000 ° K cooler than the surrounding 6000 ° K granules. Why is the spot cooler? Because it has a very strong magnetic field (3000 gauss; i.e., 15,000 times that of the Earth) that suppresses normal convection: The sunspot acts like a conical plug diverting heat flux into the neighboring photosphere outside the spot. The seven small dark features in Fig. 1 are called pores. They, too, have strong magnetic fields (1500-2000 gauss), but lack the filamentary structure (penumbra) which surrounds the dark center (umbra) of most spots. Some pores grow to become sunspots; some are old dying spots; some simply remain pores and disappear a few hours after they form. The sunspot is the most striking evidence we see on the

Sun of the interactions between convection and magnetism -- a topic we call magnetoconvection. With its strong field, it is no wonder that the sunspot is the locus of electromagnetic storms, flares and eruptions so violent that the effects are often felt at the Earth.

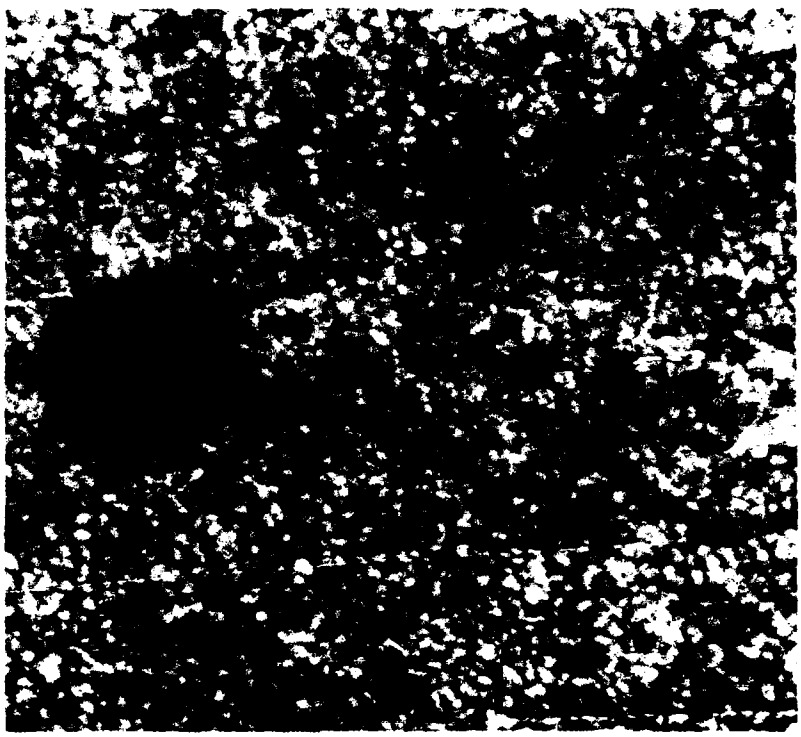

Fig. 1. High resolution solar granulation photograph from the SOUP instrument on 5 August 1985. Photo courtesy of A. Title, Lockheed Palo Alto Research Laboratory.

The solar surface is a particularly interesting place to study magnetoconvection because it is the region of the Sun where we can have equipartition of magnetic and kinetic energy density:

$$\frac{B^2}{8\pi} \approx \frac{1}{2}\,\rho v^2 \qquad (1)$$

in which v = gas velocity, B = magnetic density, and ρ = gas density which varies approximately exponentially with height in the solar atmosphere. Whether the left or right hand term in Eq. (1) is larger depends on the position under, on, or above the solar surface, and on the presence

or absence of magnetic field. In loci of strong magnetic field, like a sunspot, the magnetism dominates, and, as I have already mentioned, prevents the convective heat from coming to the surface. But away from such "active" regions that contain sunspots, in places we call the "quiet" Sun, the magnetic field is weaker and can be shoved about by the gas flows.

II. REVIEW OF EARLIER OBSERVATIONS

Ninety five years ago George Hale, father of modern observational astronomy (and founder of the Mt. Wilson and Palomar Observatories), invented the spectroheliograph [1], an instrument to photograph the Sun, not just in "white" light as with our simple granulation telescope, but in the narrow bandpass of a particular spectral line, for example, ionized calcium (Fig. 2). This ultraviolet radiation (3934Å) comes from a hotter,

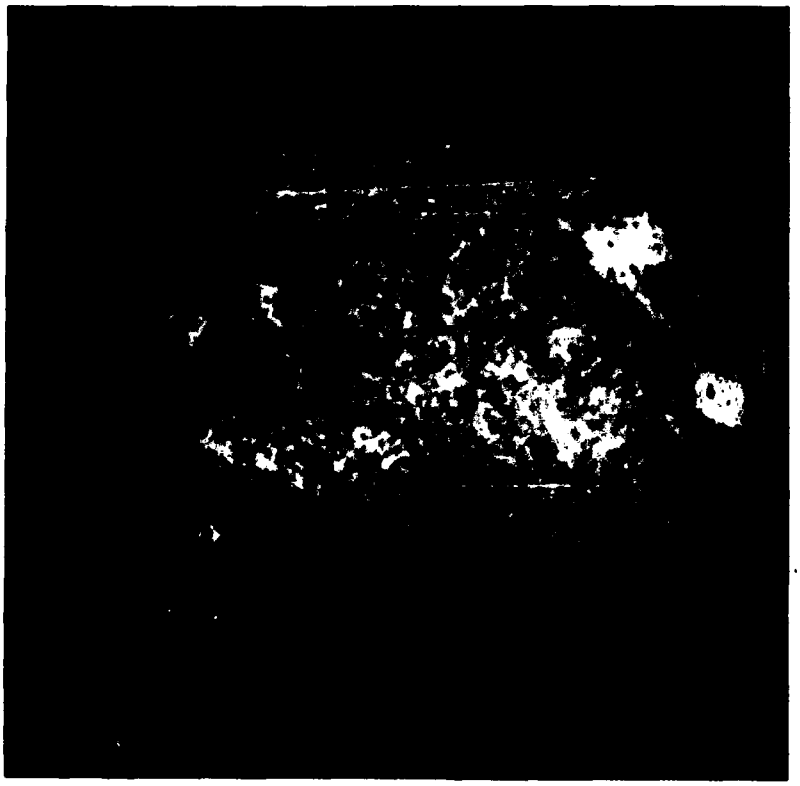

Fig. 2. Calcium (CaK) spectroheliogram of solar disk showing chromospheric network pattern. Photo courtesy of L. Gilliam, National Solar Observatory (NSO).

or
n
n/
ty Codes
Avail and/or
Dist Special
A-1 20
DTIC COPY INSPECTED 6

higher-up region of the Sun's atmosphere called the chromosphere (color sphere), and here the Sun has a strange appearance. It is covered by a mesh pattern, as though God had dropped a fish net over the Sun. We call it the chromospheric network. Note, however, that it's a rather poorly made network -- many links are missing; often one sees only bright points at the vertices of the network pattern. Fig. 3 is a greatly

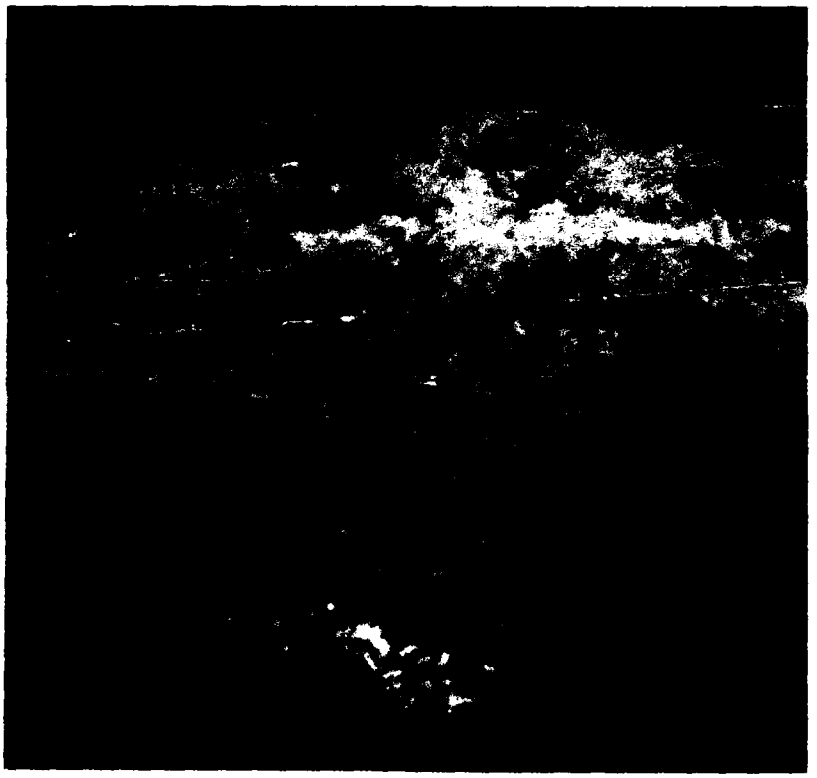

Fig. 3. Hydrogen ($H\alpha$) filtergram showing details of chromospheric network. Photo courtesy of R. Dunn, NSO.

magnified piece of this structure photographed in red hydrogen light (6563Å) with the network pattern looking every bit like hedgerows separating farmers' fields. The typical size of one of these fields is 30 Mm (or about 40", since one arcsec = 1" = 0.72 Mm), big enough to contain 2 typical sunspots, 6 Earths, or 1000 granules. Why does the Sun have this strange appearance? No one knew. In 1952 Harold and Horace Babcock at Mt. Wilson invented the photoelectric magnetograph [2] which made it possible to observe the Sun's magnetic field, and it too showed

this puzzling network pattern (Fig. 4).

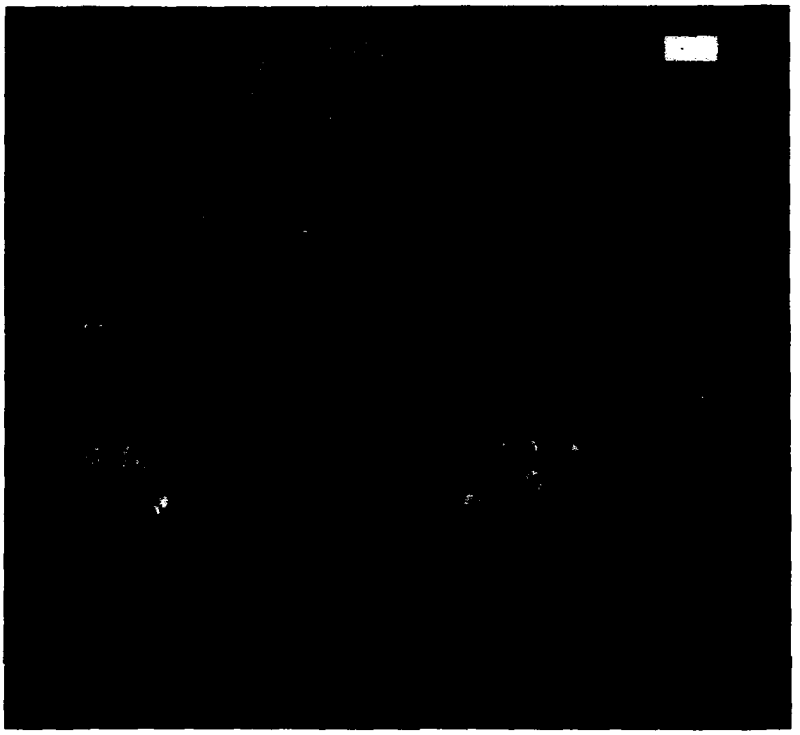

Fig. 4. Magnetogram of solar disk showing network pattern. Dark and bright patches are regions of opposite magnetic polarity. Photo courtesy of J. Harvey, NSO.

The key to solving this 70-year-old mystery was provided in 1960 at Cal Tech and Mt. Wilson by Robert Leighton, who invented a technique [3] for photographing the Sun's velocity field using the Doppler effect. Fig. 5 is such a velocity picture of the Sun in which bright features are coming toward us, dark features receding. Note that these objects are half dark, half bright, and that they don't appear at the center of the Sun. These structures can be seen more easily in Fig. 6, a larger-scale Dopplergram of a region near the Sun's limb (edge). I was a graduate student of Leighton's at that time, and a little thought led us to the conclusion [4] that we were looking at convection bubbles on the Sun -- similar to the granulation, only much bigger -- 30 Mm, so we decided to call them supergranules (note that they have the same size as the "farmers' fields" in the network pattern). If we think of a convection cell with hot gas rising at the center and spreading out when it reaches the Sun's

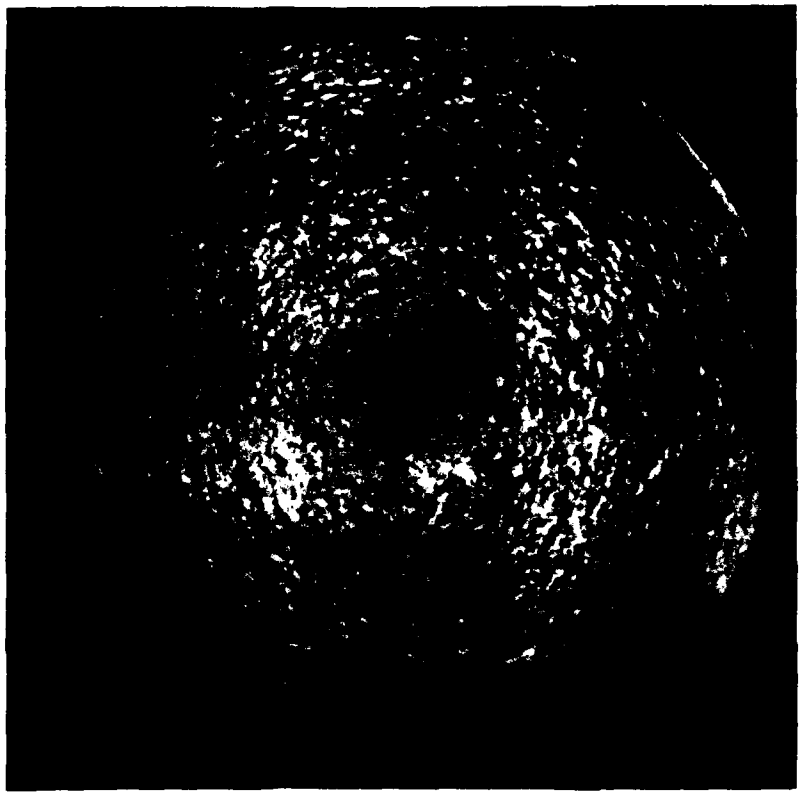

Fig. 5. Dopplergram of solar disk showing supergranules as bright (receding) and dark (approaching) velocity features.

Fig. 6. Detailed appearance of supergranules near solar limb. Polarity is reversed from Fig. 5 (dark features are receding). Photo courtesy of L. Cram, NSO.

surface (Fig. 7), we can explain the appearance of the bright and dark structures of Figs. 5 and 6. Let us consider such a cell when we look (a) directly down on it at disk center and (b) at a slant angle near the limb (cf. the schematic in Fig. 8). At disk center, the Doppler effect (which measures line-of-sight velocities) reveals only vertical motions in the cell, while near the limb it shows mainly horizontal flows. Referring back to Fig. 5, we note that no supergranule motions appear at disk center, only near the limb. The conclusions: (1) we are looking at motions which are predominantly horizontal on the Sun's surface, and (2) the bright/dark alternation of the structures indicates a radial outflow from cell center to boundary, in agreement with Fig. 7.

Discovery of the supergranulation had finally solved the problem of what causes the chromospheric network. We found that supergranules always sit inside the network, enclosed by the hedgerows. Any magnetic field inside the convection cell apparently gets pushed to the boundary where it piles up, and sometimes then slowly moves along the boundary to the corners, where it concentrates even more. It proved very difficult, however to measure details of the supergranule's structure, so difficult, in fact, that such studies were not very fruitful: Since the flow is mainly horizontal, Dopplergrams can't be used at disk center where the cell can be seen at full size. And near the limb, where Doppler signals can be measured, the cell is so foreshortened (squashed) by the slant viewing angle (cf. again Fig. 8) that details of the structure are too small to measure.

I once attempted a different technique [5] to overcome this problem. Consider the roughly 1000 granules inside each supergranule. Do they float like corks on top of the supergranular flow, and thus are carried to the boundaries of the supergranules? If so, it might be possible to use the granules as tracers of the horizontal motion within the much larger supergranule. Careful measurements of the motions of 2,300 granules showed that there was a statistical tendency for them to move toward supergranule boundaries, but an accurate description of the flow pattern was impossible with these data. Why is this measurement so difficult? Granules don't just float peacefully along as one would like. They're rude and aggressive. They often move in seemingly random directions. Some explode and destroy their neighbors. They change shape, or they disappear before they can be properly tagged. In addition, the observations are degraded by the Earth's atmosphere, which blurs, distorts, and moves the granules so that one is often unsure whether motions are real or spurious. Let me express this situation quantitatively. In the 10 s interval between photographic exposures, one expects the granules to move about 3 km. But the noise in each measurement, even under the best conditions, may be 1000 km. So the signal-to-noise ratio might typically be 0.003. No wonder the result was inconclusive. It was over 20

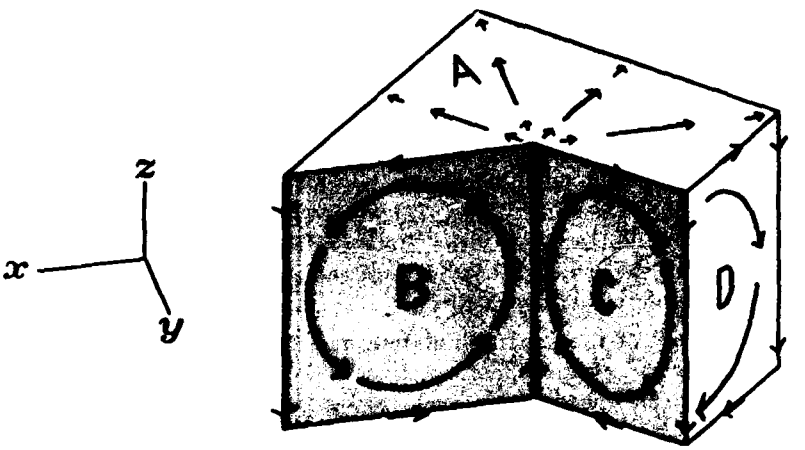

Fig. 7. Schematic model of a convection cell, with hot material rising at the center, falling at the edges.

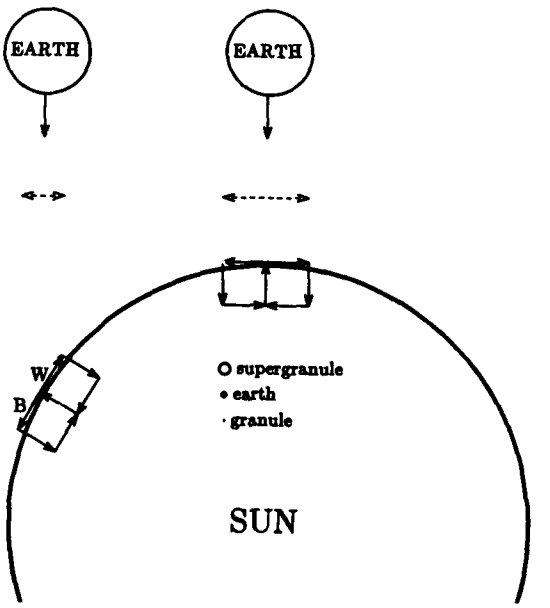

Fig. 8. Schematic model of the Sun illustrating the differing appearance to an observer at the Earth of a convection cell seen at disk center and near the solar limb. In a Dopplergram the cell appears white (W) or black (B) depending on direction of line-of-sight velocity. Dashed lines indicate observed size of a cell at disk center, and when foreshortened near the limb.

years ago that solar observers gave up on this seemingly hopeless project.

III. NEW OBSERVATIONS FROM SPACE

On 29 July 1985 NASA launched the Spacelab 2 mission as the 19th flight of the Space Shuttle. Among the 13 instruments on board was a 30 cm Cassegrain telescope and an active secondary mirror for image stabilization built by the Lockheed Palo Alto Research Laboratory [6]. The instrument was named the Solar Optical Universal Polarimeter (SOUP). One of its components was a white-light camera to photograph the solar granulation on 35mm film. In this paper we describe and analyze images from orbit 110 taken between 19:10:35 and 19:38:05 on 5 August 1985.

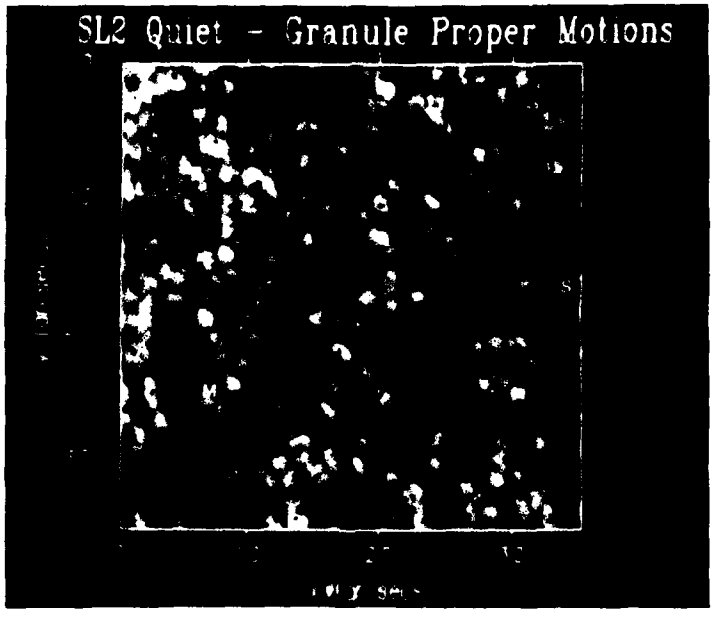

Fig. 9. A 35" by 35" section of quiet Sun photographed by SOUP. Superposed on this granulation image are vectors indicating the average motion of the granules during the 27.5 min observation. The longest vectors have velocities of about 1 km s^{-1}. The centers of a supergranule (S) and mesogranule (M) are labeled. Photo courtesy of L. November, NSO.

Frames were obtained every two seconds. The field-of-view covered an area 166" by 250". The effective wavelength band of the observations is roughly 1000Å centered on 6000Å. Magnetic data were obtained simultaneously by Cal Tech's Big Bear Solar Observatory (BBSO) in

California on the same region of the Sun from 5 August 1985, 15:25:43 to 6 August, 00:50:54, a nine-hour span surrounding the time of the SOUP observations.

These high quality granulation pictures taken by SOUP at last provided the opportunity to detect large-scale surface flows by direct displacement measurements of the local granulation intensity pattern. Compared to the 0.003 S/N ratio of the ground-based observations, the SOUP measurements have S/N ratios of 5 to 10, an improvement of 2000 to 3000 times. With the application of sophisticated local correlation tracking methods [7], it became relatively simple to make the required measurements which had previously seemed impossible. The results were just as we had suspected: The granules indeed float like corks on top of supergranules and mesogranules. (Mesogranules [8] are another type of convection cells with typical diameters of 4 to 8 Mm -- intermediate in size between granules and supergranules). We show in Fig. 9 a 35" by 35" quiet Sun area of the SOUP image [9] with clear examples of outflow from the center of a supergranule (labeled S) and a mesogranule (labeled M). Each vector represents the average motion over the 27.5 min observations of the granules in the vicinity of that arrow. That is, each vector was determined from the average motion of all the intensity features (typically 5 to 10 granules) in a 3" circular window centered at the arrow's location.

From these vectors one can compute the divergence of the horizontal surface flow:

$$D = \frac{\partial v_x}{\partial x} + \frac{\partial v_y}{\partial y} \tag{2}$$

The divergence has a positive maximum at sources such as the centers of supergranules and mesogranules where hot gas rises to the surface, and it has a minimum at sinks such as vertices of the network pattern where later, after cooling, the gas falls back down. The Sun is covered by these sources and sinks, as can be seen in Fig. 10, a 131" x 119" area of the SOUP image. There are about 40 local divergence maxima (shown as solid contours in Fig. 10) and a roughly equal number of minima (dashed contours) in an area of 10,000 square arcsec. Twelve such examples are shown in Fig. 11: The left-hand six are sources; the right-hand six are sinks. They were taken from the larger image (Fig. 10) and can be located in it because the coordinate systems correspond.

These large-scale flows also exhibit twisting motions. In analogy to Eq. (2) for the divergence, one can compute from the horizontal velocity vectors the vertical component of vorticity:

$$E = \frac{\partial v_y}{\partial x} - \frac{\partial v_x}{\partial y} \tag{3}$$

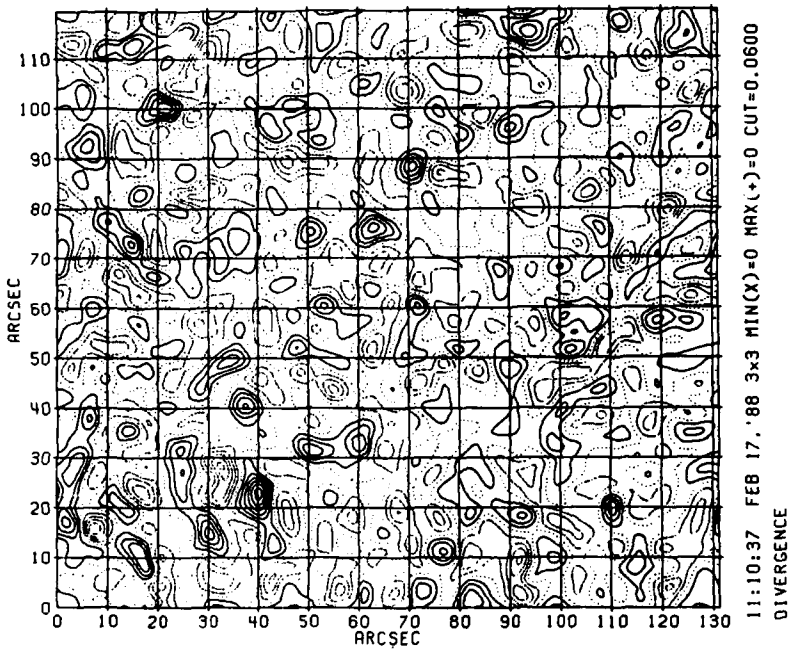

Fig. 10. A large section (131" x 119") of the SOUP image field shown as a map of the divergence of the horizontal velocity.

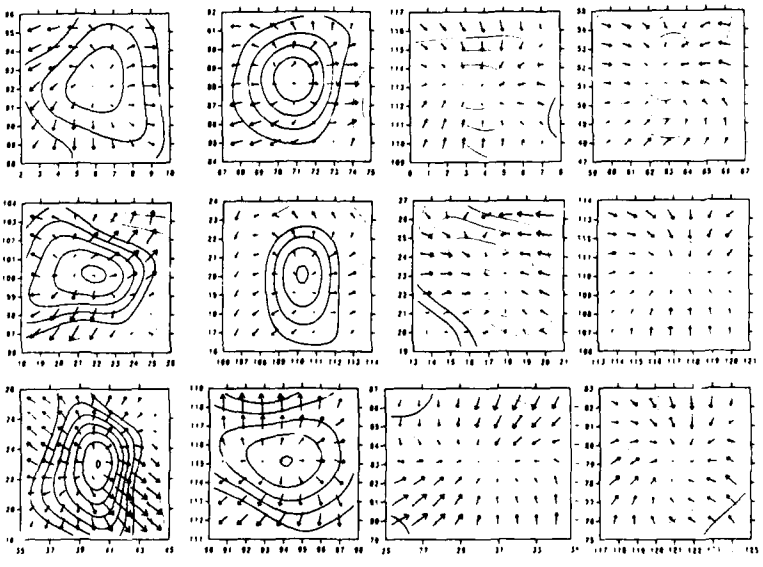

Fig. 11. Twelve examples of divergence: Sources (the six outflows on the left) and sinks (the six inflows on the right).

and calculate its value everywhere in the image. A vorticity map of the same region as Fig. 10 is shown in Fig. 12. In Fig. 13 are six clockwise

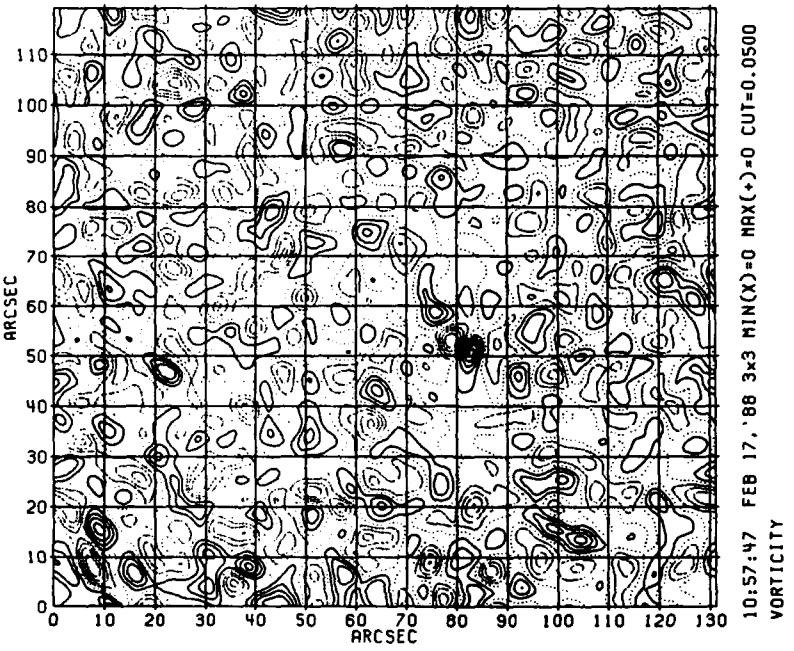

Fig. 12. Vertical vorticity of the flow in the same region of the Sun as in Fig. 10.

rotating vortices on the left, and six counterclockwise ones on the right. Particularly interesting double and triple vortex patterns are illustrated in Fig. 14. The maxima and minima of vorticity only rarely occur at the same loci as the maxima or minima of divergence. This disagrees with one's intuitive expectation that a flow would probably follow a vortical path as it is sucked into a sink. However, observation of a particularly large vortex [10] does, indeed, show this expected behavior. Since the method of local correlation tracking has, to date, been applied to only a few observations of divergence and vorticity in the solar atmosphere, further data are needed to clarify this situation.

Consider now the relation between these flows and the Sun's surface magnetic field. We pointed out in Section I that the earlier ground-based observations implied that supergranule motions pushed magnetic field to cell boundaries. These new SOUP observations, when combined with simultaneous ground-based magnetic field data from BBSO, convincingly demonstrate this to be true. We find [11] that magnetic flux elements

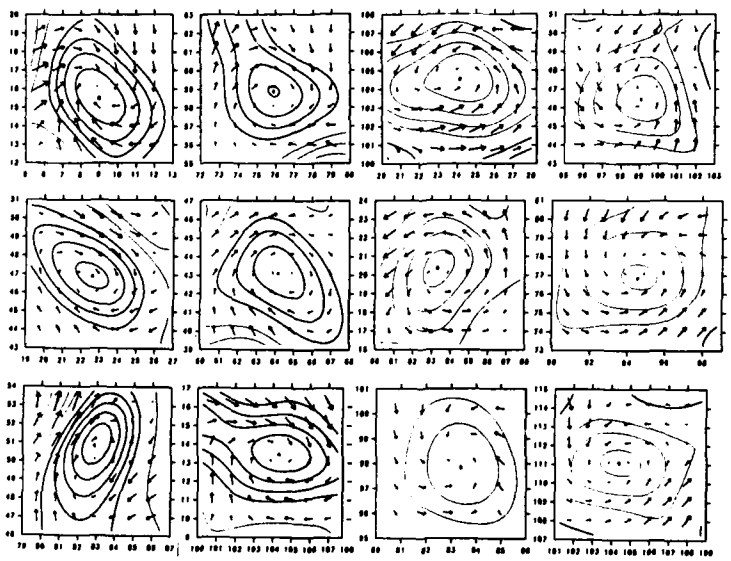

Fig. 13. Twelve examples of vorticity, showing six clockwise vortices on the left, and six counterclockwise flows to the right.

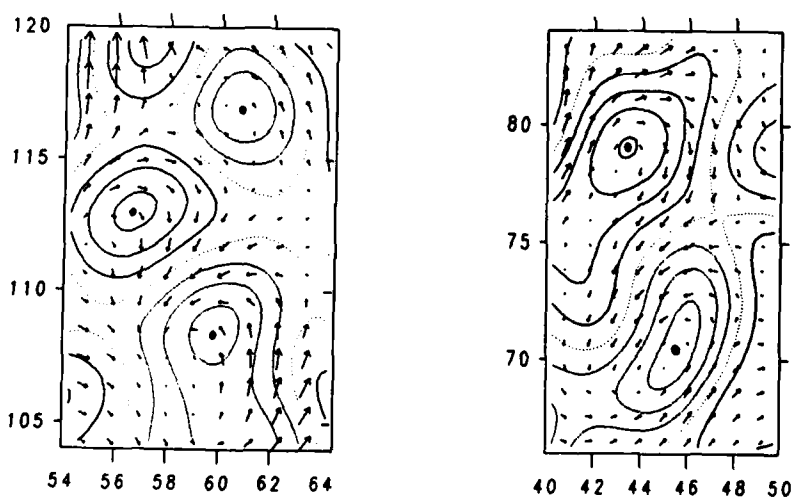

Fig. 14. Particularly interesting double and triple vortices, with adjacent cells showing counter flows.

move in patterns which are in almost perfect agreement with those of the granular corks: Both the granules and magnetic features are expelled

from the centers of mesogranules, moving first to the mesogranular boundaries and ending up at the boundaries (network) of the larger supergranules. The test particles of the motion then slowly, over a period of one to two days, concentrate into small downdrafts (sinks), although the magnetic elements apparently prefer to remain primarily as a network pattern. These results are shown most effectively by high speed (300-1000 times acceleration) cinematography, but they are summarized in Fig. 15. Here we superpose the positions of corks 8 hr after they start

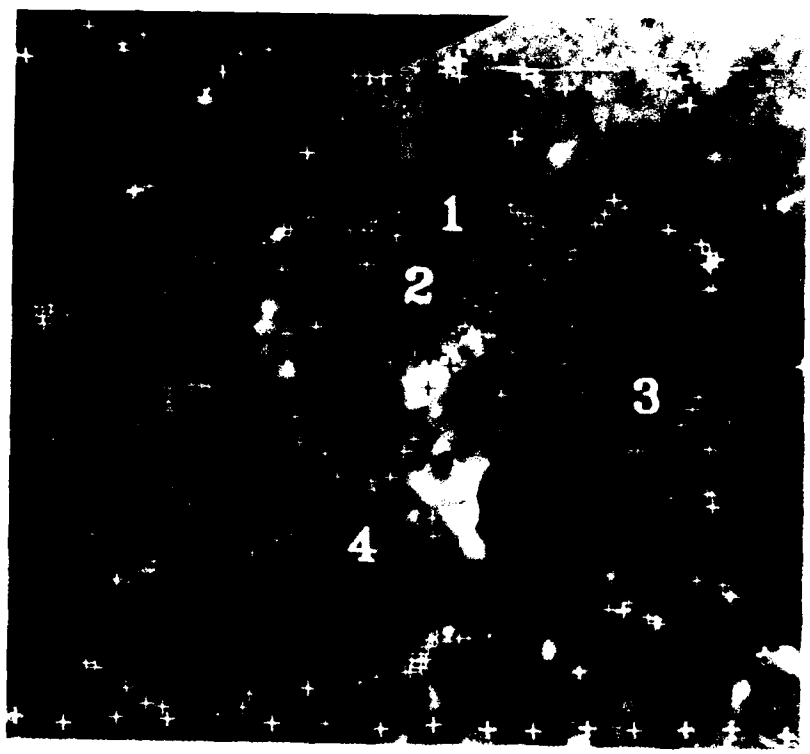

Fig. 15. Superposition of magnetic field and test particles (corks) 8 hr after corks started from a uniform distribution in the SOUP image. The cork motions were dictated by the observed horizontal flow field. Note that most corks have already reached the network regions where the magnetic field is concentrated. The centers of four flow sources are labeled. These are void of magnetic field.

from a uniform distribution and the remarkably similar magnetic field structure (dark and bright features indicate opposite field polarities).

Note, for example, that no magnetic field remains in the centers of the four labelled sources where there exist maxima of divergence.

As a final example of such magnetoconvective interactions, we show in Fig. 16 the radial outflow of granules from the sunspot of Fig. 1. The

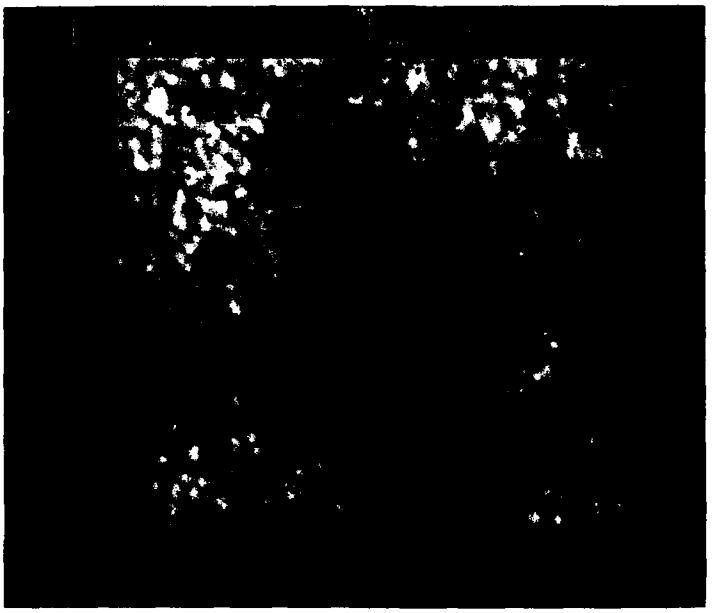

Fig. 16. Sunspot region in the SOUP image. As in Fig. 9, the vectors indicate horizontal flows in the solar surface and show that the sunspot is surrounded by an annulus of radially outflowing gas.

width of this moving annulus or "collar" immediately surrounding the sunspot penumbra is about 5", and is perhaps the most striking discovery from the SOUP data. The velocities of the outward streaming granules in the collar reach 0.5 to 1.0 km s^{-1}. Apparently, as we had suspected, the sunspot does indeed behave as a plug in the solar surface, diverting the heat flux and gas, requiring them to flow around the spot, resulting in the observed radial outflows of granules and possibly also a ring of brighter than average photosphere around the sunspot.

IV. THEORETICAL MODELING

An attempt to model these observations has begun [12-13]. We represent a convection plume by an axisymmetric source with a radial outflow described by a simple analytic function. The radial motion in

this model has a velocity:

$$v = V\left(\frac{r}{R}\right)\exp\left[-\left(\frac{r}{R}\right)^n\right], \tag{4}$$

where V and R are the strength and radius of the source, respectively. Continuity then implies that the vertical velocity w is proportional to the divergence D of the horizontal flow:

$$D = \frac{1}{r}\frac{d}{dr}(rv) = \frac{V}{R}\left[2 - n\left(\frac{r}{R}\right)^n\right]\exp\left[-\left(\frac{r}{R}\right)^n\right]. \tag{5}$$

Fig. 17 shows the variation with radius (r/R) of the normalized radial and vertical components of the velocity in an isolated plume, for n = 2, 3, and 4, with V = R = 1.

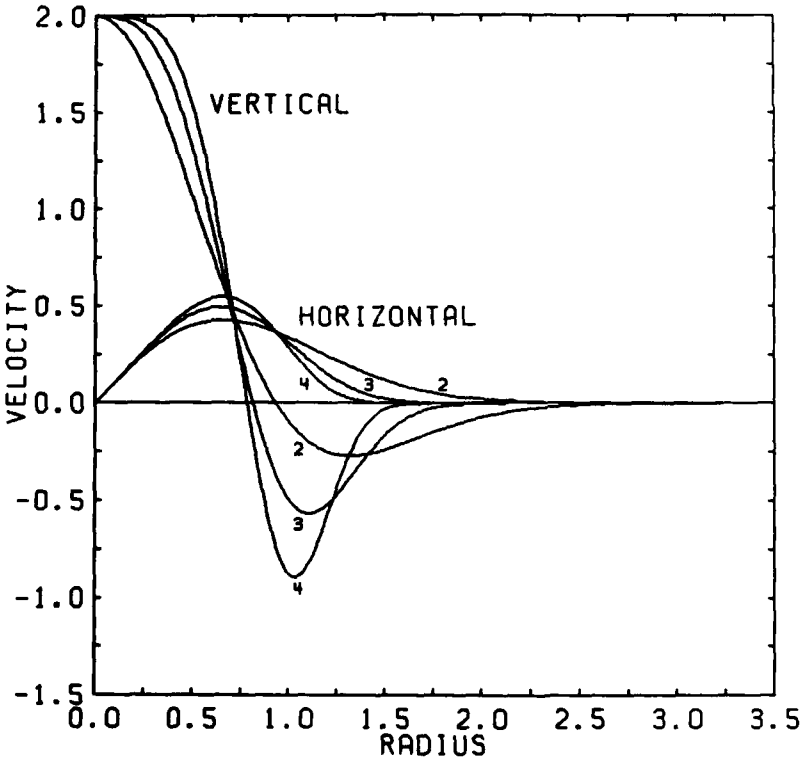

Fig. 17. Radial dependence of the horizontal and vertical velocities as function of distance from center of a plume. Velocities are shown for three values of the power n in Eq. (4) and (5).

By superposing a number of such sources we can produce regular or irregular patterns of cellular convection. This procedure has been used to simulate the large-scale horizontal flow patterns observed by the SOUP instrument. In order to model an observed velocity pattern we locate all local maxima of the divergence D in the SOUP data and fit all the significant sources with the correct maximum value D_{max} and R (the mean radius at which $D = 0$). As an example, in Fig. 18 we show radial scans (dots) from the center of the divergence peak with coordinates (37", 41") in Fig. 10. The averages of these radial scans are shown as circles (o) and can be compared with the model (Eq. 5) which yields values of D indicated by plus (+) signs. The two curves are in excellent agreement to a distance of 7", beyond which large asymmetries are created by neighboring sources and sinks. We have tested the goodness of fit between our model and the SOUP data for n = 2, 3, and 4 and conclude that n = 2 gives the most satisfactory results. This value was used in Fig. 18 and in the remainder of this analysis.

As a second test of the model, let us consider again the quiet Sun region of Fig. 9, which has x, y coordinates $95" \leqslant x \leqslant 130"$, $8" \leqslant y \leqslant 43"$, when referred to Fig. 10. We have taken the 16 strongest sources observed by SOUP in this region and fitted each source with an axisymmetric plume function as we did in Fig. 18. The resultant model flow field is compared to the SOUP data in Fig. 19. Although the real data contain sinks, streaming motions, and vorticity, none of which is included in our simple irrotational source model, nevertheless we are able to reproduce quite well the general features of the flow.

The proof of the pudding is in comparing the real and modelled cork motions, since we have shown that the SOUP corks and the magnetic structure agree very closely. In Fig. 20 (SOUP data) and Fig. 21 (model) we show the cork movements in the quiet Sun area (cf. Fig. 9) over a 48 hr period. The corks start on a uniform square grid with approximately 1" spacing at time t = 0. We show the positions of the corks after 1 hr, 2 hr, 4 hr, 8 hr, 1 d and 2 d have elapsed. In a few hours the corks move away from the centers of mesogranules and supergranules within the region. After about 8 hr they form a network outlining the mesogranular structure. The most prominent features are the supergranule S at the right of the region and the mesogranule M just below the center which we labeled in Fig. 9. At the end of a day the network is narrower, and over the next day the particles slowly migrate along the network to accumulate at junctions where the divergence D is a minimum. For the first 8 hr, the SOUP and the model corks agree very well. After 1 d, however, almost all the SOUP corks end up concentrated at sink (convergence) locations, while the model, which has no sinks, still has corks more widely distributed over the region. We conclude that our simple model, despite

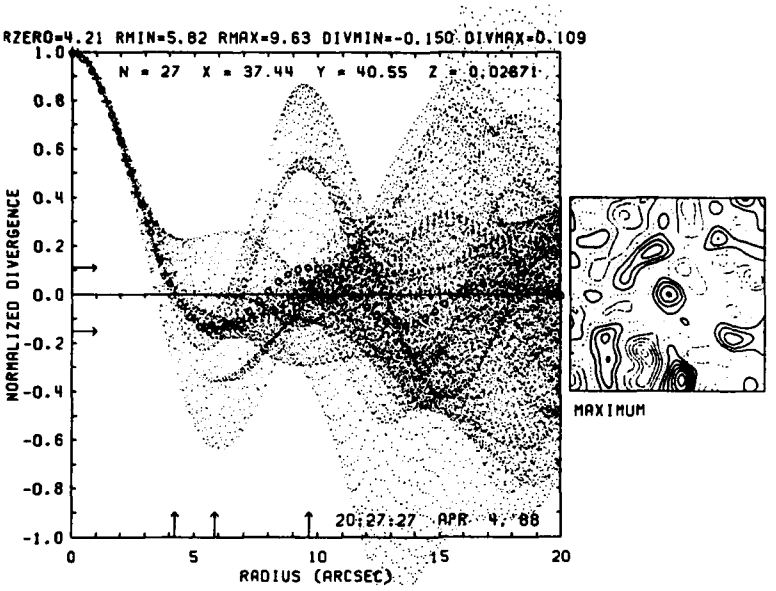

Fig. 18. Comparison between an observed SOUP source and the model. A contour map of the source is shown on the right, and can be located in Fig. 10. Radial scans from the source are shown as dots. They are noisy beyond 5" due to nearby sources and sinks. The average of all scans is shown by circles, and can be compared with the model, shown as plus signs.

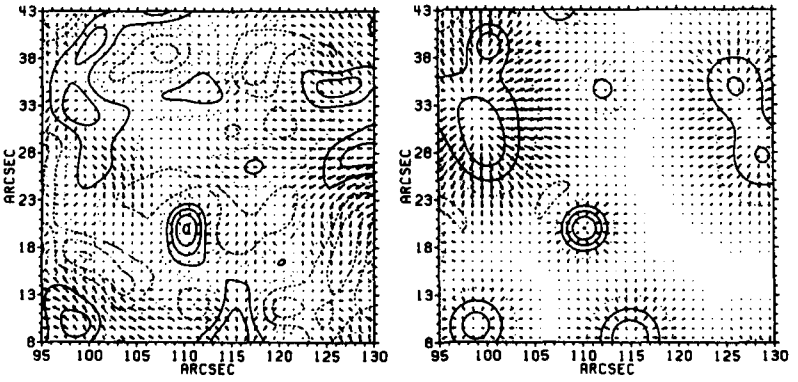

Fig. 19. Horizontal velocity (arrows) and contours of divergence (proportional to vertical velocity) for SOUP data (left) and the model (right). Solid lines indicate positive divergence (outflow); dashed lines convergences (sinks).

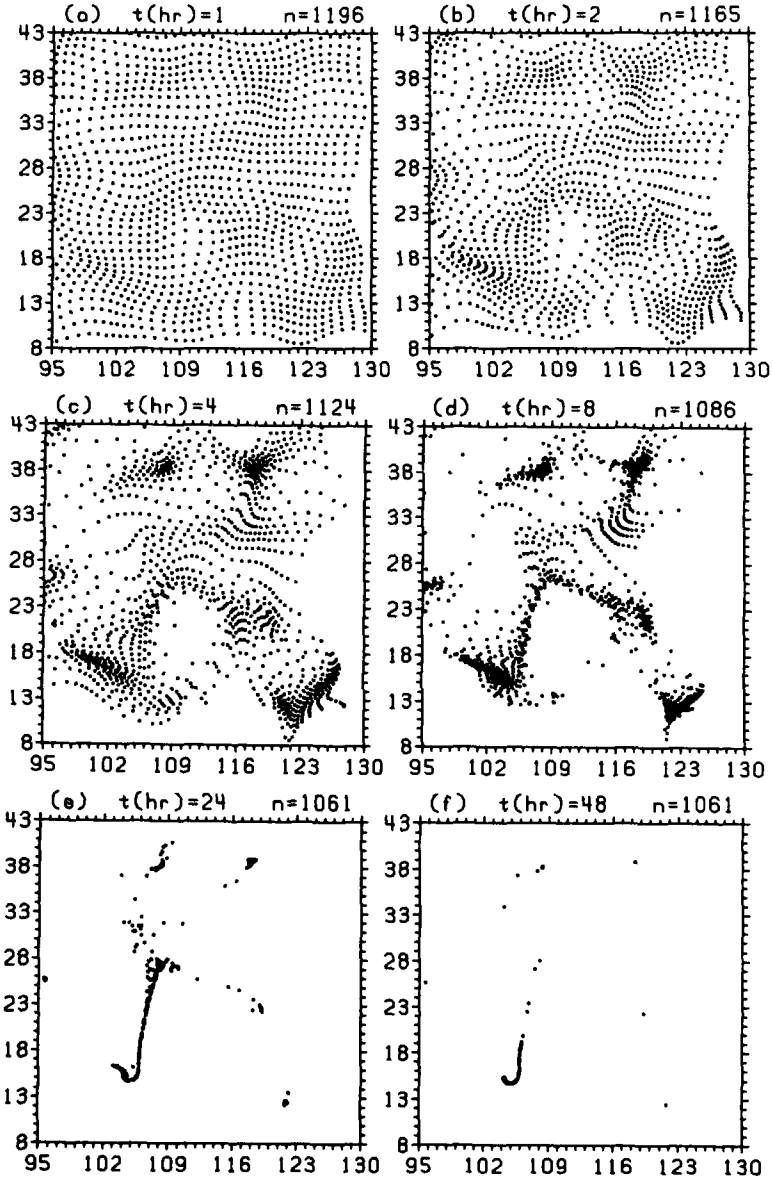

Fig. 20. Positions of test particles (corks) moving with the SOUP horizontal velocities from Fig. 19, shown 1, 2, 4, 8, 24 and 48 hr after starting from a uniform distribution. Almost all the corks end up at sink locations after one to two days.

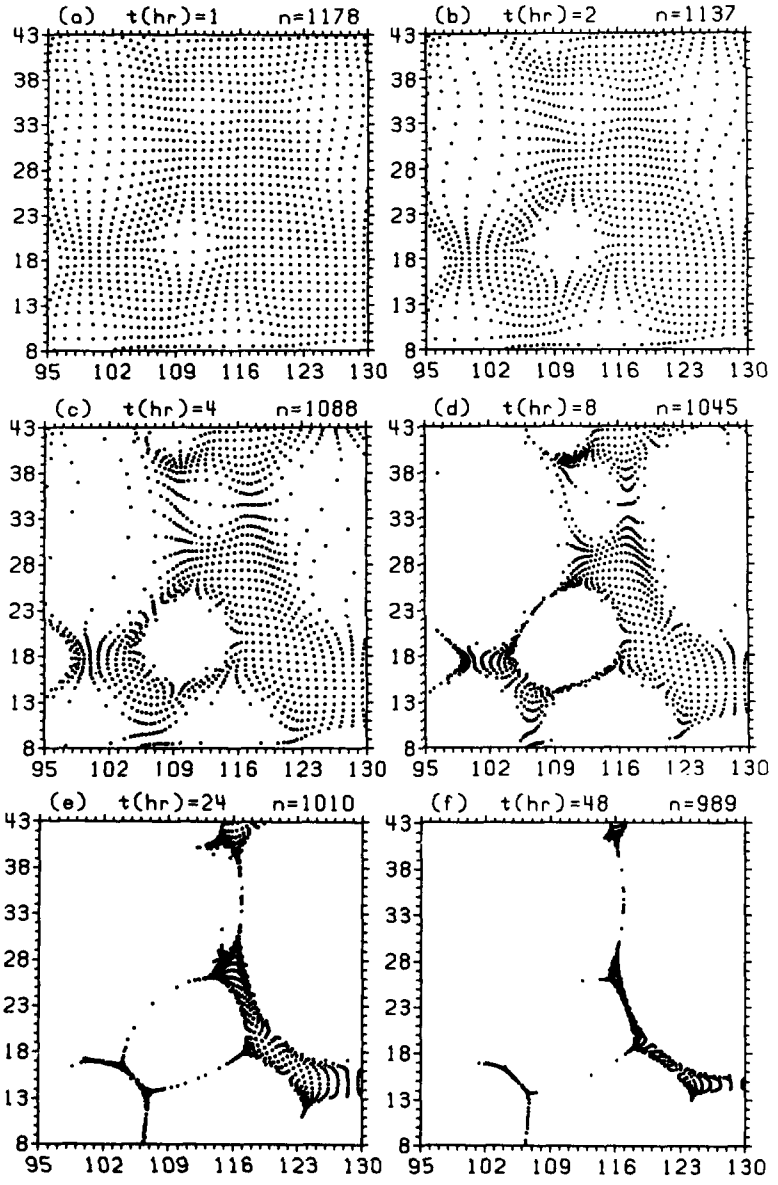

Fig. 21. Like Fig. 20, for corks moving according to the velocities of the axisymmetric plume model.

its obvious shortcomings, does a creditable job of reproducing the actual solar motions. These studies are continuing.

V. CONCLUSIONS AND SIGNIFICANCE

These simultaneous observations of white light granulation and digital magnetograms have provided some striking examples of magnetoconvection on the Sun's surface, as seen in the intimate interactions between horizontal motions and magnetic structures. We are able to demonstrate that the white light granular flow field is a nearly perfect descriptor of the motion and evolution of the magnetic field. The flow field determined from one 27.5 min SOUP measurement is an excellent indicator of the motion of the corresponding magnetic field configuration, and is valid for at least 4 hr before and after the SOUP observations. From the cork simulations we estimate that the magnetic pattern would require about 8 to 10 hr to develop, which suggests that the flow field and magnetic field have a lifetime longer than 10 hr as would be expected for large-scale supergranular structures which have 1 to 3 d lifetimes. At this level in the solar atmosphere it appears that, in general, the material motions dominate the magnetic forces; i.e., that the right-hand term of Eq. (1) is the larger. Only in the regions with strongest magnetic field (in the immediate vicinity of sunspots and pores) is the magnetic energy the bigger quantity and able to inhibit the convection.

These data also suggest to us that flow along network boundaries may be an important feature in the evolution of the magnetic field pattern. This has implications for understanding phenomena such as coronal heating and the buildup of magnetic stresses in the network. First, flow along the network boundaries will tend to mix and twist the fields on very small scales. We have measured the vertical component of vorticity of the flow field and find that at some locations it reaches values greater than 10^{-4} s^{-1}. Thus, where the vorticity is large, substantial twist can be imparted to the magnetic field in only a few hours. Such mixing and twisting will be enhanced by local displacements of the field caused by randomly-directed motions and explosions of individual granules. Second, flow along the boundaries concentrates the field into vertices. These vertices are probably stable points in the flow field, so that new supergranules may form with a vertex at the previous boundary.

For many years it has seemed clear that the tremendous and rapid release of energy in solar flares must be due to electromagnetic forces, probably through magnetic reconnection when stressed magnetic fields suddenly return to lower-energy states. It has also appeared likely that such stresses build up through the translational and twisting motions of the footpoints (located in and below the photosphere) of magnetic arches which extend upward into the solar corona. Thus these new observations

from Spacelab 2 of the horizontal flows at the solar surface are extremely valuable to theorists who have argued that dissipation and heating in magnetic regions depend critically on the spatial scale of the twisting of magnetic flux tubes [14-16]. Recent studies [17] have used 3-D models to show how shearing photospheric flows might build up the energy of a magnetic arcade until it becomes unstable, forms current sheets, and then reconnects in the corona with rapid release of magnetic energy. Our hope is, of course, that from such observations as we have described in this paper, we will learn how to identify the locations of maximum stress where instabilities and heating are most likely to occur, and thus eventually understand where and when solar flares will be triggered.

ACKNOWLEDGEMENTS

I would like to thank Dr. L. November of the National Solar Observatory and Prof. N. Weiss of the University of Cambridge for their invaluable help in the analysis and interpretation of these data, and other members of the SOUP research team (A. Title, T. Tarbell, K. Topka, R. Shine, and S. Ferguson) and Prof. H. Zirin of the California Institute of Technology for their key roles in many aspects of the work described herein.

REFERENCES

[1] Hale, G. 1892, *Astr. & Astr.-Phys.*, **11**, 407.
[2] Babcock, H. and Babcock, H. 1952, *P.A.S.P.*, **64**, 282.
[3] Leighton, R., Noyes, R., and Simon, G. 1962, *Ap.J.*, **135**, 474.
[4] Simon, G., and Leighton, R. 1964, *Ap. J.*, **140**, 1120.
[5] Simon, G. 1967, *Zs. Ap.*, **65**, 345.
[6] Title, A., Tarbell, T., Simon, G., and the SOUP Team 1986, *Adv. Space Res.*, **6**, 253.
[7] November, L. and Simon, G. 1988, *Ap. J.*, **333**, in press, Oct 1.
[8] November, L., Toomre, J., Gebbie, K., and Simon, G. 1981, *Ap. J. (Letters)*, **245**, L123.
[9] November, L., Simon, G., Tarbell, T., Title, A., and Ferguson, S. 1987, in *Proc. 2d Workshop on Theoretical Problems in High-Resolution Solar Physics*, NASA Conf. Pub. 2483 (Washington, DC: NASA), ed. G. Athay, p. 121.
[10] Brandt, P., Scharmer, G., Ferguson, S., Shine, R., Tarbell, T., and Title, A. 1988, *Nature*, in press.
[11] Simon, G., Title, A., Topka, K., Tarbell, T., Shine, R, Ferguson, S., Zirin, H., and the SOUP Team 1988, *Ap. J.*, **327**, 964.

[12] Simon, G. and Weiss, N. 1986, *B.A.A.S.*, **18**, 990.
[13] Simon, G. and Weiss, N. 1988, *Ap. J.*, submitted.
[14] Van Ballegooijen, A. 1986, *Ap. J.*, **311**, 1001.
[15] Parker, E. 1972, *Ap. J.*, **174**, 499
[16] Parker, E. 1983, *Ap. J.*, **264**, 642.
[17] Mikic, A., Barnes, D., and Schnack, D. 1988, *Ap. J.*, submitted.